JOURNAL OF MATERIALS SCIENCE 27 (1992) 1514–1520

Cyclic oxidation of Haynes 230 alloy

FEN-REN CHIEN*, R. BROWN
Materials Laboratory in the Department of Chemical Engineering, University of Rhode Island, Kingston, RI 02881, USA

The cyclic oxidation of Haynes 230 alloy (Ni–Cr–W–Mo alloy) was investigated in air at three different temperatures, 871, 982 and 1093 °C. Studies indicated that during cyclic oxidation, protective scales formed which were predominantly Cr_2O_3, with Kirkendall voids formed both at the scale/alloy interface and grain boundaries. Intergranular oxides were observed at temperatures above 982 °C while internal oxide particles were found above 1093 °C. Both intergranular and internal oxides were identified as aluminium oxide. A 50 μm chromium-depleted zone developed after 70 h exposure at 1093 °C and was accompanied by disastrous scale spalling. The lowest chromium concentration within the depleted zone was 14 wt% which still provided a sufficient supply of chromium for development of a continuous Cr_2O_3 rich scale. Decarburization was observed at the higher temperature of 1093 °C, and a carbide-free zone developed. Also, it was found that Haynes 230 is subject to a sensitization process. At the lower exposure temperature of 871 °C, large amounts of chromium carbide formed preferentially at the grain boundaries. While at the surface region chromium carbide precipitation occurred at the twin boundaries.

1. Introduction

The protective scales formed on most high-temperature alloys during oxidation consist of either Cr_2O_3 or Al_2O_3 [1–3]. Chromium is a key element for oxidation resistance, provided temperatures do not exceed 950 °C for extended periods of time. At temperatures above 950 °C, chromium vaporizes and liberates CrO_3 instead of forming the more desirable barrier oxide scale rich in chromia (Cr_2O_3) or spinel (MCr_2O_4) [1, 4, 5]. However, below 950 °C in Ni–Cr alloys, a critical chromium content of about 10–15 wt % determines the nature of the external oxide type. Above the critical level, a Cr_2O_3 rich scale formed, while at lower concentration the external scale is NiO-rich [5–7]. The most abundant oxide in the layer is not necessarily the most thermodynamically stable one, but in addition depends on the diffusional flux of the metal species towards the surface as well as mechanical factors. Chromium and aluminium-layers are usually observed below scales in the alloys resulting from diffusion to form a surface oxide. Aluminium provides excellent oxidation resistance by forming Al_2O_3. This is thermodynamically more stable than Cr_2O_3 and less prone to vaporization effects. However, poor adherence to the substrate results from high aluminium ion migration and, in comparison with Cr_2O_3, is a problem. The poor adherence of alumina scales has been shown to be improved by small additions of oxygen-active elements such as yttrium, lanthanum, zirconium and hafnium [4, 8–12]. Also, those additives might reduce the diffusion rate of Al^{3+} in Al_2O_3 which is much faster than in Cr_2O_3 because active element oxides, i.e. Y_2O_3, may block the diffusion of cations. Therefore, additives might suppress the void formation in the interface between the scale and matrix and thereby increase scale–metal adhesion.

Strafford *et al.* [10] indicated that the effect of small additions of aluminium can be beneficial even when the concentration is insufficient to allow external scale formation. In this case, it is considered that precipitation of aluminium oxide particles may occur internally in the alloy, perhaps leading to the formation of a barrier layer underneath the main scale, i.e. Cr_2O_3. In contrast, Stott *et al.* [6] also found that internal and intergranular oxides probably form in Ni–Cr–Al alloys, and those oxides are mainly α-Al_2O_3. The occurrence of intergranular oxidation can lead to a mechanical weakening of the substrate due to short-circuit grain boundaries providing paths to form α-Al_2O_3.

In this study, Haynes 230 alloy, a recently developed nickel-base superalloy (Ni–Cr–W–Mo alloy) material used in the combustion region of jet engines, was cyclically oxidized. Its composition is listed in Table I.

In the maximum range of combustion operating temperature, around 871–1093 °C, tensile and compressive stresses are induced by the different expansion coefficients between the scale and the matrix when cooled or heated rapidly under the jet engine flight service cycles. It is known that cyclic thermal exposure causes more serious oxidation than static thermal exposure. The purpose of this study was

* *Present address*: Division of Engineering, Brown University, Providence, RI 02912, USA.

0022–2461

TABLE I Composition (wt %) of Haynes 230 alloy

Ni	Cr	Mo	W	Fe	Co	Si	Mn	C	Al	B	La
Bal.	22	2	14	3[a]	5[a]	0.4	0.5	0.10	0.3	0.005	0.02

[a] Maximum amount.

therefore to investigate the cyclic oxidation behaviour of this newer alloy to determine its mechanisms of oxidation and scale growth in the temperature range 871–1093 °C.

2. Experimental procedure

Haynes 230 alloy with the composition shown in Table I was used in cyclic oxidation tests. The oxidation samples were small 1.25 cm discs, 0.3 cm thick. Before testing, the surface of the discs were wet ground on silicon carbide paper down to 600 grit and cleaned in acetone.

2.1. Apparatus

A vertical quartz tube furnace with a reversible motor above it was used in this experiment. Attached to the motor was a pulley connected to a platinum wire on which disc specimens were suspended. The lower end of the tube furnace was sealed to avoid serious heat convection. Using a personal computer with software, the motor was controlled to pull the discs up into the air and lower them into the furnace according to a programmed cycle. The period of cyclic oxidation was 30 min in the furnace and 5 min at room conditions. The furnace temperature was set at three different operating temperatures: 871, 982 and 1093 °C.

2.2. Metallographic examination and compositional analysis

After cyclic oxidation, the microstructure and crystal morphology of the oxidized surface was observed by scanning electron microscopy (SEM). In addition, energy dispersive X-ray analysis (EDS) was conducted to identify the composition of the surface and all new layers formed during the test. The disc sample was then cross-sectioned by a diamond saw and mounted in epoxide resin. The mounted specimens were wet ground on SiC paper down to 1200 grit, and then polished to a 0.3 μm alumina paste finish. After etching, SEM was employed to observe scales and EDS to identify compositions. The etching solution consisted of 30 ml HCl, 10 ml HF and 10 ml HNO_3. The etching time for the samples was 4 min.

3. Results

3.1. Weight change behaviour

To investigate long-term exposure, a fresh set of Haynes 230 discs were exposed for 300 h at three different temperatures listed above. Under 871 and 982 °C exposures, the weight change curves were not smooth, as shown in Fig. 1, which implied the scales cracked or spalled slightly and small amount of local oxidation occurred. In contrast to the weight change behaviour under 871 and 982 °C heat treatments which showed some spalling but not enough to cause weight loss, after 24 h exposure at 1093 °C, the scale spalled disastrously causing a weight loss equal to the original weight gain. After 130 h exposure the scale began to thicken again. It should be noted that the first 24 h data, i.e. weight gain, recorded during the 300 h exposure tests were identical with shorter exposure tests of only 24 h confirming the initial data.

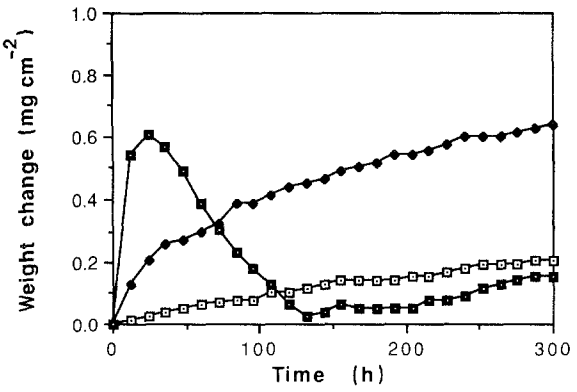

Figure 1 Weight change behaviour of the cyclic oxidation in air for 300 h at (□) 871 °C, (◆) 982 °C, (■) 1093 °C.

3.2. Surface microstructure and composition

At 871 °C, after 24 h thermal cyclic exposure, individual cubic-like crystals ($\approx$ 1 μm) covered the surface. Increasing the thermal exposure time to 300 h, the surface microstructure changed to non-uniform agglomerations, which are similar to Fig. 2. Between the agglomerations some microcracking was evident. A comparison of the EDS analysis results indicated that the initially formed NiO layer after 24 h exposure spalled or was replaced by Cr_2O_3 due to chromium preferentially diffusing outward to the surface. The initially formed WO_3 was absent after 300 h exposure and it was assumed tungsten vaporized due to its high volatility. Therefore, after 300 h thermal exposure, a highly chromium-rich oxide scale was observed.

At 982 °C, after the first 24 h thermal exposure, extrusive agglomerations covered the surface, as shown in Fig. 2. Apparently in Fig. 2, defects (microcracks) existed around the agglomerations. Those defects may result from the thermal stresses induced by the different coefficients of thermal expansion between oxide layer and substrate, and thereby provide the path for oxygen penetration. As the thermal exposure time was extended to 300 h, the microstructure was much the same as that after 24 h thermal exposure.

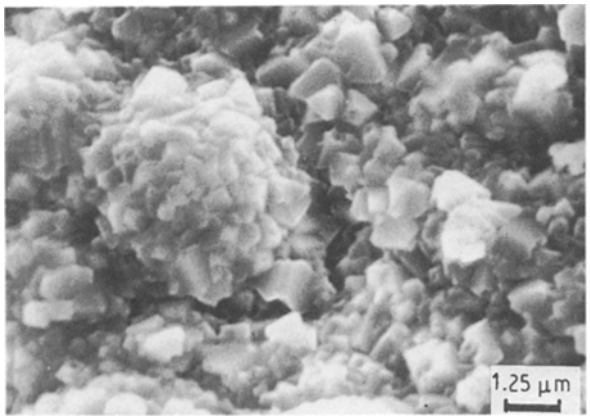

Figure 2 Surface microstructure after 24 h cyclic exposure at 982 °C in air.

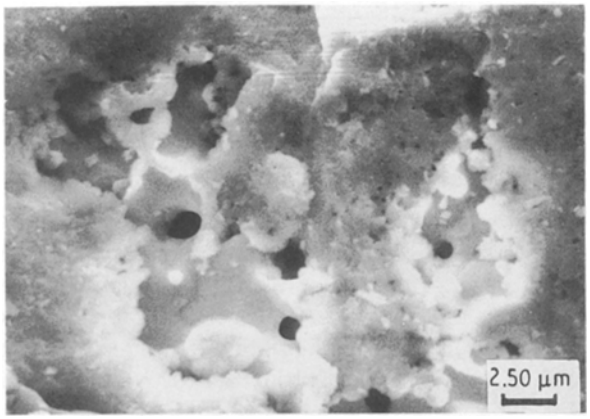

Figure 3 Surface spalling spot after 24 h cyclic exposure at 1093 °C in air.

However, some large individual extrusive agglomerations cracked diametrically, possibly as a result of growth and thermal stresses.

EDS analysis indicated that the average composition of the top scale surfaces at all different exposure times for 982 °C were much the same as each other, and essentially consisted of chromium-rich oxides with no tungsten and a small nickel content.

At 1093 °C, essentially, after 24 h thermal treatment the agglomerated nature of microstructure of the surface was the same as that after 982 °C thermal exposure, with the additions of some exposed surface areas devoid of any coarse crystalline features. As noted for both 982 and 1093 °C cases, the extrusive agglomeration crystals were highly chromium-rich oxides. However, some spalled areas were found on the surface scale, Fig. 3. The base areas exposed by spalling were still chromium-rich but with higher nickel content than the scale. Upon further examination of the base areas at higher magnification, Fig. 3, some voids were found. The voids were suspected evidence of the selective oxidation of chromium. The formation of the voids resulted from preferential chromium diffusion outward to the surface to form Cr_2O_3, leaving vacancies which coalesced together to form voids by the Kirkendall effect. On the top surface, those voids look like small holes. As the exposure time increased, i.e. 70 h, the exposed areas from spalling covered with very fine highly chromium-rich crystals. At this stage, weight change behaviour in Fig. 1 implied a large amount of scale spalling, but the average compositions of the surface still retained the scale composition of highly chromium-rich oxides. As the exposure time was increased to 200 h, the weight change transformed from losing to gaining. No matter how much scale spalled off, the surface was still chromium-rich.

At 1093 °C heat treatment, three stages were chosen to examine surface compositions. Those stages were at 24, 70, and 300 h exposure. EDS analysis results indicated that all of these three surfaces were chromium-rich. In comparison to their weight change behaviour, analysis results implied that there was abundant chromium content in the alloy to support the continual formation of Cr_2O_3.

3.3. Cross-sectioned microstructure and composition

Generally, after cyclic oxidation in air, only one chromium-rich oxide scale was formed on the surface. However, at thermal treatment temperatures in excess of 982 °C, intergranular and internal oxidations were observed. The formation of voids, the development of chromium-depleted zones and tungsten carbide-free zones were also examined.

At 871 °C, the chromium-rich oxide scale formed uniformly on the surface and it adhered firmly to the substrate. Small cavities existed between the oxide film and the matrix in which ligaments formed to connect the scale and the matrix. The composition of the scale is similar to the top surface. For short-term exposure, the scales retained some nickel and tungsten content; for long-term exposure, the scales were purified to highly chromium-rich oxide. After 120 h cyclic exposure at this temperature, tungsten carbide particles were retained immediately underneath the scale, Fig. 4. It implied that little carbon, if any, was removed by decarburization. At this temperature, no intergranular or internal oxides were observed.

At 982 °C, the oxide scales were thicker and more non-uniform than after 871 °C exposure; few intergranular oxides along the grain boundaries were

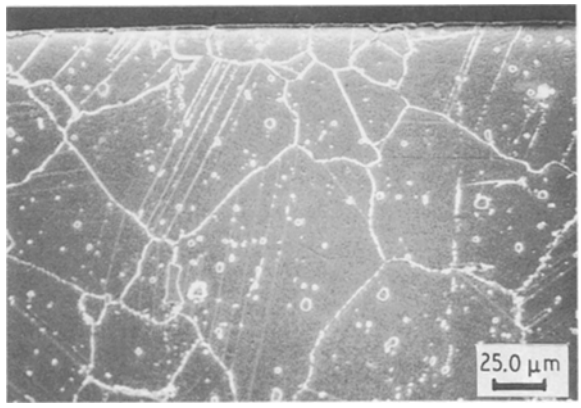

Figure 4 Microstructure of scale after 24 h cyclic exposure at 871 °C in air. Note the precipitate decorated grain boundaries and tungsten carbide particles near the external scale.

found. These intergranular oxides were aluminium-rich oxides but still retained high chromium and nickel contents. At this temperature, no internal oxide particles were found.

At 1093 °C, 24, 70 and 300 h exposure samples were examined. The typical 300 h exposure microstructure is shown in Fig. 5a and b. The weight change curve indicated that at these times, different processes were occurring. After 24 h exposure, some spalled areas were obvious. Cavities were found not only at the scale/matrix interface, but also at the grain boundaries. Many more intergranular oxides were found than after 24 h exposure at 982 °C. These intergranular oxides were highly aluminium-rich oxides.

For the 70 h exposure, large amounts of scale were spalling and a newly developed scale, adherent to the substrate, Fig. 5b, was formed beneath the spalling film. Fig. 5b is a good example to illustrate how the newly developed scale might form. When the scale spalled, separation along the scale/alloy interface allows oxygen to penetrate, reacting with the freshly exposed substrate metal to form a new scale on the exposed metal surface below the previously existing scale. The weight change behaviour implied, at this stage, that the scale was spalling catastrophically. The development of scale and continual spalling consumed considerable amounts of chromium. EDS analysis indicated that the newly formed scale maintained a highly chromium-rich oxide. The EDS microprobe trace of chromium concentration beneath the scale is presented in Fig. 6. The depth of chromium depletion in the alloy beneath the external scale after 70 h was found to be 50 μm. The minimum chromium concentration close to the external scale was determined to be 14 wt % Cr. This result suggests that the chromium concentration was retained above the critical chromium concentration in the alloy, in order for selective oxidation of chromium. Voids could be found both at the scale/alloy interface and at the grain boundaries. The void formation could be due to the selective oxidation of chromium. Large intergranular oxides formed preferentially along the grain boundaries and just beneath the scale, Fig. 5b. Within the grains and beneath the scale, dispersed internal oxides could also be found. Those intergranular oxides and internal oxides were aluminium-rich oxides.

The microstructure after 300 h exposure was similar to the structure after 70 h exposure, but the chromium-depleted zone was extended to 95 μm and the minimum chromium concentration was increased to be 16 wt %. The chromium concentration–depth profile after 300 h is shown in Fig. 6. At this stage, the newly developed chromium-rich oxide scale, Fig. 5b, adhered firmly to the substrate. More internal oxide particles and a larger internal oxidation zone were observed than after 70 h exposure. It is suggested that the chromium outward diffusion rate was blocked by the internal Al_2O_3 particles close to the scale. As a result of blocking the chromium from going into the scale so rapidly, the minimum chromium concentration which occurred in the metal close to the newly formed scale was increased to 16 wt %. As the bulk material continues to provide the source of chromium for the formation of the external Cr_2O_3, but the transport rate is blocked by the internal oxide particles, a buildup of chromium occurs.

Apparently, in the surface regions both after 70 and 300 h exposure, tungsten carbide disappeared, as can be seen in Fig. 5a. Depletion of tungsten carbide was not found at 871 and 982 °C. It suggested that tungsten carbide dissolved into the γ-phase matrix because of the depletion of carbon by a decarburization process allowed by the increased spalling of the scale at the elevated temperature, exposing fresh metal surface and thus providing the paths for the carbon to diffuse through.

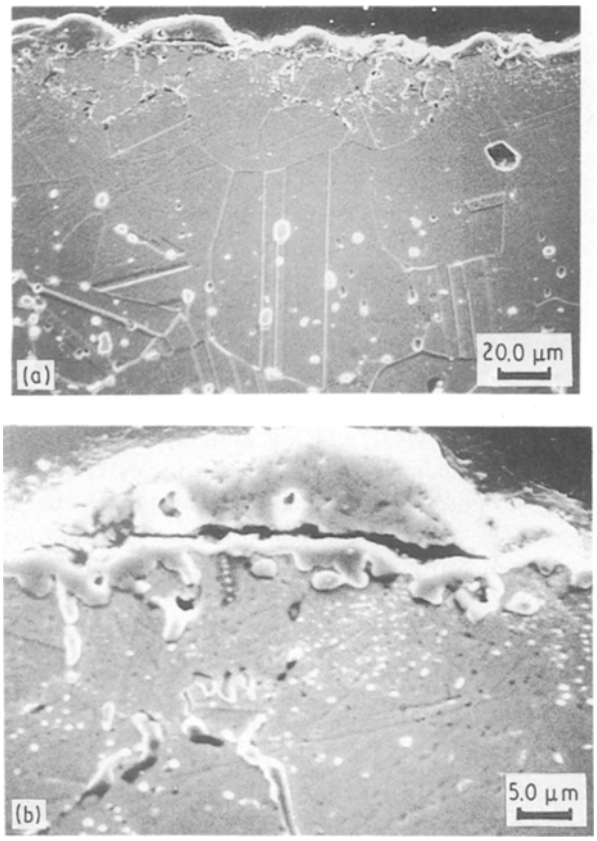

Figure 5 Typical microstructure of scale after 300 h cyclic exposure at 1093 °C in air. (a) Internal and intergranular oxides. Also a tungsten carbide-free zone was developed. (b) A higher magnification of (a) with new adherent scale and large intergranular and internal oxides.

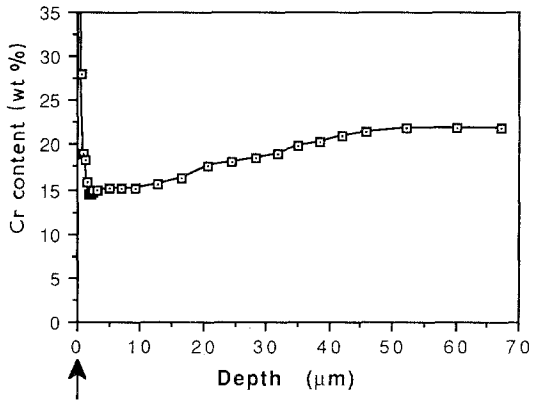

Figure 6 EDS of microprobe trace of chromium concentration after 70 and 300 h cyclic exposure at 1093 °C in air.

3.4. Formation of chromium carbide

Within the as-received material, except for a low number of individual, separate tungsten carbide particles located randomly in the grains and grain boundaries, no continuous precipitation was found along the grain boundaries. It is interesting that after 871 and 1093 °C cyclic exposure, the microstructures in the bulk are different. A large amount of precipitation formed along the grain boundaries after 24 h cyclic exposure at 871 °C. These precipitates were identified by EDS as chromium carbides, in comparison to the original tungsten carbides. The microstructure of the chromium carbide is shown in Fig. 7a and b. The morphology of the chromium carbide is somewhat like a dendritic structure growing from boundaries into grains. Extending the exposure time to 120 or 300 h at 871 °C did not alter the microstructure, and the dendritic carbide was maintained.

On the other hand, after 24 h cyclic exposure at 1093 °C, the carbide morphology changed to small particles precipitated along grain boundaries instead. These particles were identified by EDS as chromium carbide. Extending the exposure time to 300 h at 1093 °C, reactions resulted in some chromium carbide particles disappearing at the grain boundaries in coarsening.

It should be noted that precipitation occurred along twin boundaries only which intersected or were close to the free surface at 871 °C. The microstructure is shown in Figs 4 and 8, and should be compared with the 1093 °C structure shown in Fig. 5. These precipitates along the twin boundaries were chromium-rich compounds which were suggested to be chromium carbide, because its EDS results were similar to the dendritic carbide at the grain boundaries. Within the region near the free surface, slightly less chromium carbide in the grain boundaries was observed than the bulk centre matrix. It indicated that the carbon content was marginally decreased in the region near the free surface after oxidation. Therefore, some decarburization during the heat treatment is expected, if the continuous scale formed at 871 °C is removed exposing fresh unprotected surface. Such was the case at 1093 °C where clear evidence of spalling and decreased carbon in the form of tungsten carbide particles near the surface was found.

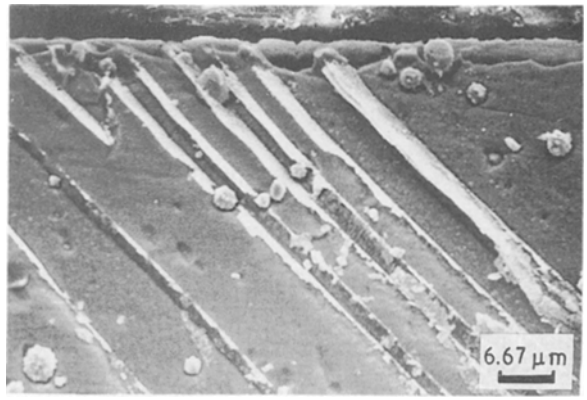

Figure 8 Precipitation formed at twin boundaries close to the free surface after 24 h cyclic exposure at 871 °C in air.

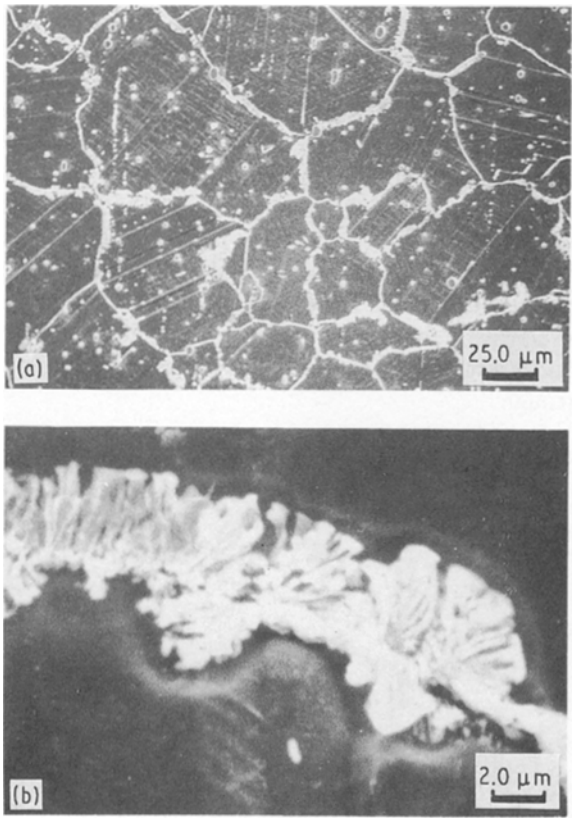

Figure 7 (a) Dendritic chromium carbide preferentially formed at the grain boundaries after 24 h cyclic exposure at 871 °C in air. (b) A higher magnification of the dendritic chromium carbide.

4. Discussion

Haynes 230 superalloy (Ni–22Cr–2Mo–14W–3Fe–5Co–0.4Si–0.5Mn–0.1C–0.3Al–0.005B–0.02La) has a high content of chromium and tungsten. Although, in simple binary Ni–Al alloys, the addition of chromium to a level of 10% drops the amount of aluminium required to form and maintain the external Al_2O_3 from 10% to around 5% from a gettering effect [13], the aluminium concentration in Haynes 230 alloy is too low to affect the external oxide formation initially. Thus, as the fresh discs were placed into the high-temperature furnace, NiO, Cr_2O_3 and WO_3 formed. Consequently, WO_3, which is a highly volatile oxide, escaped and cannot accumulate on the external surface. NiO and Cr_2O_3 then compete with each other to dominate external layer formation. A critical chromium concentration exists of about 10–15 wt % determining the nature of the external oxide type which is rich in Cr_2O_3 at higher concentrations and rich in NiO at lower concentrations [5–7]. In Haynes 230 alloy, the chromium content is far above the critical chromium concentration needed for the formation of Cr_2O_3 external oxide. For the long-term exposure at 871 °C, highly chromium-rich oxides were found on the external layer. In contrast, some nickel oxides were detected for short-term exposure. It is suggested that two possible paths can explain the purification of the external layer to Cr_2O_3.

1. Initially a $NiO + Cr_2O_3$ layer formed then spalled after several cycles.

2. Cr_2O_3 is much more stable than NiO. The initially formed NiO will be reduced by chromium through the displacement reaction [14]

$$3\,NiO + 2\,Cr(\text{in alloy}) = 3\,Ni(\text{in alloy}) + Cr_2O_3$$

For case 1, substantial surface spalling and a large weight loss would be evident at the 24 h stage of exposure. Only limited spalling was found at this stage at 871 °C, suggesting that reduction of NiO was the mechanism of Cr_2O_3 formation.

Usually, if an easily oxidized element is trapped below a protective layer, internal or intergranular oxidation may take place if sufficient oxygen can diffuse through the scale. Normally, the concentration of the easily oxidized element is very low, i.e. aluminium in Haynes 230 alloy is 0.3 wt %. For a thermal exposure temperature and time of 982 °C and 24 h, and higher, intergranular oxides composed of highly aluminium-rich oxides were observed. It is suggested that some degree of spalling is necessary to allow oxygen to diffuse into the substrate to react with aluminium trapped below the scale. The more coherent scale at 871 °C did not allow enough oxygen penetration for oxide formation. The development of internal oxidation required increased temperature and exposure time. Grain boundaries are the preferential sites as they can provide short-circuit paths for aluminium and oxygen diffusion, and can accommodate higher oxygen solubility than the grains. Therefore, grain boundaries provide the sites for internal oxidation.

It is believed that void formation between the scale and substrate or the cavities found in the exposed areas are both due to the selective oxidation of chromium (Kirkendall effect). It also should be noted that some voids were found along the grain boundaries. The reason for this might be due to the defect structure in grain boundaries providing short-circuit paths for outward diffusion of chromium. Meanwhile, the formation of intergranular aluminium-rich oxides which were found in the grain boundaries at the higher exposure temperatures reduced in Kirkendall voids, and acted as pegs of the outer Cr_2O_3-rich scale increasing the outer scale's mechanical adhesion and stability. The observation can be seen in Fig. 5a. In general, intergranular aluminium-rich oxides increase the adherence of the scales. It therefore appears that processes detrimental to a coherent scale are required to increase local scale adherence by Al_2O_3 formation. Al_2O_3 does not form unless sufficient oxygen can penetrate through cracks and spalled areas of scales. Therefore, some loss of scale and a poor scale is necessary for peg formation which may itself lead to local attack.

The weight change behaviour in Fig. 1 indicated that, at 1093 °C cyclic exposure, the development of scale and continual spalling consumed considerable amounts of chromium. Nevertheless, there exists a wide chromium-depleted zone which can supply chromium to develop new scale. EDS analysis indicated that the newly formed scale maintained a highly chromium-rich oxide. Also the newly formed scale adhered firmly to the substrate and the scale growth rate was reduced by the internal aluminium-rich oxide particles blocking the outward diffusion of chromium.

Haynes 230 alloy is solution heat-treated in the range of 1177–1246 °C and rapidly cooled or water-quenched for optimum properties. Before any heat treatment, only tungsten carbide particles are dispersed in the as-received materials. As the discs were heat treated at 871 °C, a large amount of dendritic chromium carbide precipitated along the grain boundaries. Meanwhile, as the discs were heat treated at 1093 °C, only a small amount of particulate chromium carbide could be found dispersed along the grain boundaries. These phenomena are similar to those associated with stainless steel Type 304 (Fe–18Cr–8Ni–0.08C). When 304 steel is heat treated above 982 °C and cooled down rapidly, little, if any, chromium carbide particles can be found. If it is cooled down slowly through a sensitizing range (427–874 °C) [15], a precipitate of dendritic chromium carbide is formed preferentially at the grain boundaries. This dendritic chromium carbide [15] in 304 steel is similar to that observed in Haynes 230 alloy, as shown in Fig. 7b. This observation indicates that the stainless nickels such as Haynes 230 are also subject to sensitization which can lead to grain-boundary corrosion, which is a serious problem in sensitized stainless steel. Fig. 7b not only shows the grain-boundary carbide phase but shows some intergranular corrosion. After the sample was polished, it was etched in hydrochloric acid etch solution. The zone of metal near the carbides is depleted in chromium which was used to form the particles. The zone is, therefore, anodic to the bulk grains as well as the carbide particles. The acid etch therefore dissolves the metal around the carbide at an accelerated rate.

A large amount of chromium carbide formed preferentially at the grain boundaries after cyclic exposure at 871 °C, but little was found at 1093 °C. For the surface region, after 24 h cyclic exposure at 871 °C, chromium carbide not only preferentially formed at the grain boundaries, but also at twin boundaries at or near the free surface, Fig. 8. During lower temperature oxidation, some dissolved carbon can diffuse outward through the γ phase to the metal surface where it reacts with oxygen to form monoxide. This is the driving force for free carbon diffusing through the surface. Therefore, the grain boundaries and twin boundaries provide the short-circuit path for carbon diffusion. Thus, free carbon may be concentrated at the grain boundaries and twin boundaries near the free surface. As the protective scale grows and thickens, it may block the diffusion of carbon from the free surface and thereby reduce the carbon diffusion rate. Eventually, the concentrated carbon at the grain boundaries and twin boundaries attract chromium, diffusing to form surface scale, to form chromium carbide, which then retards decarburization by decreasing the mobility of carbon. Thus, chromium carbide has been developed both at the grain boundaries and the twin boundaries near the surface region.

Duh and Wang [16] have shown that for Fe–Mn–Al–C alloys, the early stages of oxidation are dominated by a carbon-induced oxidation at the

lower temperature (800–950 °C). On the other hand, the oxidation of metallic elements predominates in the early stages of oxidation at the higher temperature. In this study, contrary results were obtained. At the lower temperature (871 °C) cyclic exposure, even after 120 h oxidation, tungsten carbide particles were retained right underneath the scale, as shown in Fig. 4. It implied that most of carbon was maintained inside the substrate. But, only after 70 h cyclic exposure at 1093 °C, a 40 μm tungsten carbide-free zone was developed close to the free surface. It indicated that decarburization rate at 1093 °C is higher than at 871 °C. There are two possible reasons accounting for the above observation. First, the scale formed at 871 °C was very uniform and protective and no obvious cracks or spalling spots can be seen. It implied that carbon was blocked by the protective scale. For 1093 °C cyclic exposure, many crack channels and spalling spots formed, as shown in Figs 3 and 5b. The spalling areas provided the paths for carbon diffusing outward to the free surface. Second, at lower temperature exposure, large amounts of free carbon were trapped to form chromium carbide and cannot diffuse outward.

5. Conclusion

Scales owe their protective properties to Cr_2O_3. The initially formed NiO might have spalled or preferentially been replaced by Cr_2O_3 and nickel itself back into the alloy, and the initially formed WO_3 escaped by vaporization. Intergranular aluminium-rich oxides were observed only at the exposure temperature above 982 °C. As the exposure temperature was increased to 1093 °C, more intergranular oxidation sites than at 982 °C were found. Internal aluminium-rich oxide particles were observed only at the temperature of 1093 °C and an exposure time of more than 70 h. The internal particles may block the diffusion of chromium and thereby reduce the formation rate of the protective Cr_2O_3-rich scale. Grain boundaries could provide the short-circuit diffusion path for either cations (i.e. Cr^{3+} and Al^{3+}) or oxygen. Chromium tended to diffuse outward through the grain boundaries and then created Kirkendall voids. Intergranular aluminium-rich oxides filled in voids and acted as the pegs of the outer Cr_2O_3-rich scale. In general, the intergranular aluminium-rich oxides increase the adherence of the Cr_2O_3-rich scale. After 70 and 300 h exposure at 1093 °C, the chromium-depleted zones were up to 50 and 95 μm and the lowest chromium concentrations were decreased down to 14 and 16 wt %, respectively. They still can provide the chromium source to develop continuously the Cr_2O_3-rich scale. At the higher exposure temperature of 1093 °C, a wide tungsten carbide-free zone developed, which is associated with decarburization. Haynes 230 alloy is also subject to sensitization. Only at lower temperature (871 °C) exposure, is a large amount of dendritic chromium carbide formed preferentially at the grain boundaries. In the surface region, chromium carbide not only preferentially formed at the grain boundaries, but also at the twin boundaries.

Acknowledgements

Many helpful discussions with Dr T. J. Rockett, Chemical Engineering Department, University of Rhode Island, are gratefully acknowledged. Provision of laboratory in the Department of Chemical Engineering is also acknowledged.

References

1. D. P. WHITTLE and H. HINDAM, in "Corrosion-Erosion-Wear of Materials in Emerging Fossil Energy Systems", edited by A. V. Levy (NACE, Houston, TX, 1982).
2. G. C. WOOD and F. H. STOTT, in "Proceedings of NACE Conference on High Temperature Corrosion", San Diego, March 1981.
3. K. P. LILLERUD and P. KOFSTAD, *J. Electrochem. Soc.* **127** (1980) 2397.
4. P. ELLIOTT, *Mater. Perform.* **4** (1989) 57.
5. N. BIRKS and G. H. MEIER, "Introduction to High Temperature Oxidation of Metals" (Arnold, London, 1983) pp. 107–24.
6. F. H. STOTT, G. C. WOOD, Y. SHIDA, D. P. WHITTLE and B. D. BASTOW, *Corr. Sci.* **21** (1981) 599.
7. G. C. WOOD, F. H. STOTT, D. P. WHITTLE, Y. SHIDA and B. D. BASTOW, *ibid.* **23** (1983) 9.
8. K. N. STRAFFORD, *High Temp. Technol.* **1** (1983) 307.
9. J. C. PIVIN, C. ROQUES-CARMES, J. CHAUMONT and H. BERNAS, *Corr. Sci.* **20** (1980) 947.
10. K. N. STRAFFORD, P. K. DATTA, A. F. HAMPTON and P. MISTRY, *ibid.* **29** (1989) 673.
11. A. B. ANDERSON, S. P. MEHANDRU and J. L. SMIALEK, *J. Electrochem. Soc.* **132** (1985) 1695.
12. C. A. BARRETT, A. S. KHAM and C. E. LAWELL, *ibid.* **128** (1981) 25.
13. T. N. RHYS-JONES, *Corr. Sci.* **29** (1989) 623.
14. P. KOFSTAD, "High Temperature Corrosion" (Elsevier Applied Science, London, 1988) pp. 339, 362.
15. M. A. STREICHER, in "Stainless Steel '77", edited by R. Q. Barr (AMAX, London, 1977) pp. 1–34.
16. J. G. DUH and C. J. WANG, *J. Mater. Sci.* **25** (1990) 268.

Received 7 November 1990
and accepted 10 April 1991